Local order in hydrogenated amorphous germanium thin films studied by extended x-ray absorption fine-structure spectroscopy

1997 J. Phys.: Condens. Matter 9 5875

(http://iopscience.iop.org/0953-8984/9/27/017)

J. Phys.: Condens. Matter **9** (1997) 5875–5888. Printed in the UK PII: S0953-8984(97)83013-5

Local order in hydrogenated amorphous germanium thin films studied by extended x-ray absorption fine-structure spectroscopy

G Dalba†, P Fornasini†, R Grisenti†, F Rocca‡, I Chambouleyron§ and C F O Graeff§‖

† Dipartimento di Fisica dell'Università di Trento and Istituto Nazionale di Fisica della Materia, I-38050 Povo (Trento), Italy

‡ Centro CNR-ITC di Fisica degli Stati Aggregati, I-38050 Povo (Trento), Italy

§ Instituto de Física, Universidade Estradual de Campinas, UNICAMP, CP 6165, 13083-970 Campinas, Brazil

Received 3 April 1997

Abstract. The effect of hydrogenation on the local order in amorphous germanium has been studied by EXAFS. Measurements have been carried out on sputtered a-Ge:H films with hydrogen concentrations of 0, 7, 10, and 15 at.%, as a function of temperature in the range 11–300 K. The first-shell EXAFS data were analysed by the ratio method based on cumulant expansion. The asymmetric distributions reconstructed from cumulants are in very good agreement with a parametrized distribution obtained by other researchers using calculated phase-shifts. For the unhydrogenated a-Ge (deposited at 220 °C), increases of the interatomic distance, 0.018 ± 0.03 Å at 11 K, static disorder, $\sigma^2_{stat} = (1.9 \pm 0.3) \times 10^{-3}$ Å^2, and thermal disorder, $\Delta\nu_E = 0.28$ THz, have been found with respect to those for c-Ge. Both the static and the thermal disorder are smaller than for an evaporated sample (deposited at 160 °C) previously studied. The insertion of hydrogen in a-Ge produces a sharp reduction of the interatomic distance, static disorder, and asymmetry of the distribution already at the lowest H concentration (7%); then these parameters decrease almost linearly when the hydrogen content increases. No appreciable influence of hydrogenation on the thermal disorder has been detected.

1. Introduction

In recent years, there has been a growing interest in hydrogenated amorphous germanium (a-Ge:H) films, due to the improvement in the deposition conditions [1]. Hydrogenated germanium is a natural candidate for device applications requiring a small band gap, such as bottom-layer solar cells in tandem structures and infrared detectors. Hydrogen plays a fundamental role in the optoelectronic and structural properties of tetrahedrally bonded amorphous semiconductors. H atoms remove some of the weak bonds, and passivate dangling orbitals, both relaxing the structure and improving the electronic properties. Hydrogen is also thought to be intrinsically connected with metastability effects observed for a-Si:H [2] and a-Ge:H [3]. However, very little is known about the effects of hydrogen on the short-range structure.

‖ Present address: Departamento di Física e Matemática, FFCLRP-USP, Avenida Bandeirantes 3900, 14040-901 Ribeirão Preto, Brazil.

0953-8984/97/275875+14$19.50

Knowledge of the atomic structural arrangement in amorphous semiconductors such as a-Ge:H is very important to the understanding of their physical properties: the electronic band structure, and the optical and transport properties are related to the network structure. The influence of the network structure on the stability of the physical properties of a homogeneously disordered network of a-Ge:H has been demonstrated experimentally [4]. It is usually accepted that the local structure of a-Ge:H is predominantly that of a disordered tetrahedrally coordinated network; it is also known that the incorporation of H in amounts of the order of 10 at.% influences the network connectivity, and reduces the number of point defects. However, there is only a relatively poor quantitative knowledge of the short-range order in terms of bonding length, static and thermal disorder, and asymmetry of the distance distribution function.

The aim of this paper is to study the role of H as regards the local structure of the a-Ge network. We begin by analysing the structure of an a-Ge film prepared by sputtering; then we investigate the influence of H on the local order in three samples of a-Ge:H with different concentrations of H: 7, 10, and 15 at.%. The structural technique that we use is that of making measurements of the EXAFS (extended x-ray absorption fine structure). Such a technique has been much used to investigate a-Ge [5, 6], and a-Ge-based systems. In particular, it was also applied, in its standard formulation, to some a-Ge:H films by Stern and co-workers [7]. The standard method is based on the harmonic approximation, which assumes the distance distribution to be gaussian. Although this approach has provided original information, and led to the criticism of some conclusions obtained via x-ray scattering concerning the a-Ge first-shell coordination number [7], it is rather inaccurate when dealing with asymmetric distributions of distances. The first EXAFS investigation which assumed a non-gaussian distribution, and determined the centroid, variance, and third moment of the first-nearest-neighbour distribution in a-Ge:H at room temperature, was done by Wakagi *et al* [8].

The present work is a study of the EXAFS at the K edge of Ge as a function of temperature. We go beyond the harmonic approximation, applying the cumulant method to the EXAFS data analysis [9, 10]. This method allows us to characterize the local order of the first coordination shell of Ge atoms in terms of cumulants, i.e., of parameters which describe the distance distributions, such as the average interatomic distance, the Debye–Waller factor, and asymmetry parameters. The temperature dependence allows us to determine separately the thermal and static disorder. A preliminary short account of this work has been presented in reference [11].

The paper is organized as follows. Section 2 contains some experimental notes concerning the sample preparation and x-ray absorption measurement. In section 3 we show the EXAFS signals and give some details of the data analysis. The results are presented in section 4, together with a discussion. A summary and conclusions are reported in section 5.

2. Experimental details

The amorphous germanium samples were deposited on a 3 μm Al foil by rf sputtering a pure crystalline Ge target in an atmosphere of Ar, which was mixed with a 10% hydrogen partial pressure in the case of the hydrogenated compounds. To vary the hydrogen content in the sample, the deposition temperature was changed from 75 to 220 °C. The unhydrogenated a-Ge sample was deposited at 220 °C. Crystalline silicon wafers were also used as substrates for transmission spectra measurements in the near infrared and infrared. In order to get a good EXAFS signal-to-noise ratio, the sample thickness x was optimized for an edge jump at the K edge of Ge, $\Delta\mu x = 1.0$, where μ is the absorption coefficient. The sample

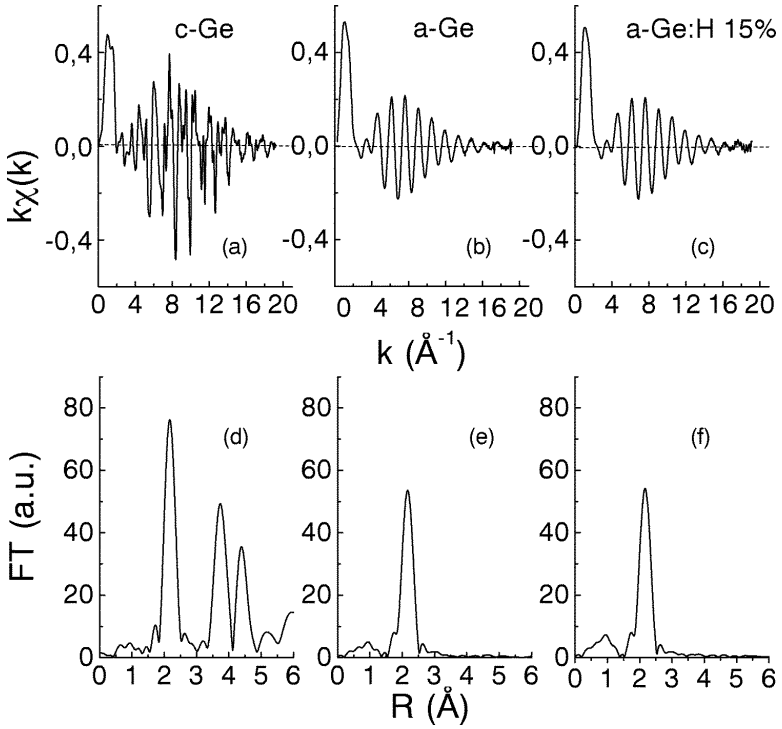

Figure 1. EXAFS signals of (a) c-Ge , (b) a-Ge, and (c) a-Ge:H 15 at.%, and their Fourier transforms ((d), (e), and (f), respectively). The measurements were made at 11 K.

thickness and hydrogen content were estimated from the interference pattern of the NIR–IR transmission spectra and from the integrated absorption of the Ge–H wagging vibration [12, 13], respectively.

The EXAFS measurements were carried out at the D42 experimental station of the storage ring DCI at the LURE laboratories in Orsay, in the transmission mode, up to a transferred momentum of $k = 20$ Å^{-1}. The beam energy of DCI was 1.85 GeV, and the maximum stored current ≈300 mA; the monochromator was a silicon channel-cut crystal with reflecting (331) faces. Absorption spectra were recorded by two ionization chambers filled with air. The sample temperature was changed from 11 to 300 K in seven steps; the temperature uncertainty was estimated to be less than 2 K. A c-Ge powdered sample was measured at 11 K as a reference for the data analysis.

3. EXAFS signals and data analysis

The data analysis was performed along the same lines as in a previous paper dedicated to the EXAFS study of c-Ge and an evaporated a-Ge film [14]. Here we will just recall the most relevant parameters, and add some remarks.

The values of the photoelectron wavevector k were calculated with respect to an energy origin E_0 set at the maximum of the first derivative of each spectrum. The refinement of the k-scale of each spectrum was done by carefully aligning the edges to within 0.1 eV. A mismatch of 0.1 eV in the edge positions of two spectra is reflected in a difference in the interatomic distance of about 0.001 Å.

The EXAFS function was determined for each spectrum as

$$\chi(k) = [\mu(k) - \mu_1(k)]/\mu_0(k)$$

where $\mu(k)$ was the experimental absorption coefficient, $\mu_1(k)$ a spline polynomial best fitting the average behaviour of $\mu(k)$, and $\mu_0(k)$ a smooth function with a Victoreen-like slope (equal for all spectra), and absolute values normalized to the experimental absorption jump. In figures 1(a), 1(b), and 1(c) the EXAFS signals $k\chi(k)$ for c-Ge, a-Ge, and a-Ge:H (15 at.%) at 11 K are shown respectively. The spectra of the amorphous samples are less structured than the c-Ge one, suggesting that only the first interatomic shell contributes to the EXAFS signal.

The $k^3\chi(k)$ functions were Fourier transformed in the range $k = 2.7$–16 Å^{-1} using a 10% Hanning window. In figures 1(d), 1(e), and 1(f) the amplitudes of the Fourier transforms (FT) for c-Ge, a-Ge, and a-Ge:H (15 at.%) at 11 K are reported; they confirm that only the first coordination shells of the amorphous films contribute to the EXAFS, unlike the case for the crystalline compound, where contributions of the first three shells are evident. The absence of contributions from the second and outer shells in the a-Ge EXAFS, even at the lowest temperatures, has been attributed to the relatively high degree of static disorder and the lack of low-k information [15]; the additional effect of destructive interference between the second-shell and multiple-scattering signals has recently been pointed out [16]. The amplitudes of the first-shell peaks of the FT of the amorphous films are smaller than that of the corresponding peak of c-Ge because of the static disorder.

The first-shell contribution to the EXAFS was isolated by Fourier back-transformation of the corresponding peak. The phases $\Phi_s(k)$ and amplitudes $A_s(k)$ of the first-shell EXAFS signals at different temperatures were separately analysed by the cumulant expansion method truncated at the fourth-order term:

$$\Phi_s(k) - \Phi_r(k) = 2k\,\Delta C_1 - \frac{4}{3}k^3 C_3$$

$$\ln\frac{A_s(k)}{A_r(k)} = \ln\frac{N_s}{N_r} - 2k^2\,\Delta C_2 + \frac{2}{3}k^4 C_4$$

where the index r labels the reference spectrum of c-Ge measured at 11 K, for which the harmonic approximation was assumed valid, and the index s labels the unknown system. The analysis of the amplitudes is based on three free parameters: the coordination number, and the second and fourth cumulants; while the analysis of the phases is based on two parameters: the first and third cumulants. The temperature dependence of the polynomial coefficients C_i is largely independent of the interval of k used for the fitting, and is consistent with the expected first-order behaviour of the cumulants (Einstein-like, parabolic, and cubic for ΔC_2, C_3, and C_4, respectively). This suggests that the convergence of the cumulant series is fast enough to guarantee that the first four cumulants are sufficient to describe the EXAFS signal within 16 Å^{-1} up to 300 K; the polynomial coefficients can then be identified as the cumulants of the effective distribution of the first-shell distances. Besides this, the assumption of harmonic behaviour for the 11 K reference is reasonable, and the analysis gives absolute values of the third and fourth cumulants directly.

4. Results and discussion

EXAFS analysis gives the cumulants C_i of the effective distribution of interatomic distances $P(r, \lambda) = \rho(r)\exp(-2r/\lambda)/r^2$ (λ being the photoelectron mean free path). The cumulants C_i^* of the real distribution $\rho(r)$ are in principle different [17]. For the second- and higher-order cumulants the difference is generally negligible, in particular when only relative

comparisons are made between systems with a comparable degree of disorder, as in the present case. For the first cumulant, however, the difference cannot be neglected, and to a first approximation [9, 17]

$$C_1^* = C_1 + \frac{2C_2}{C_1}\left(1 + \frac{C_1}{\lambda}\right). \tag{1}$$

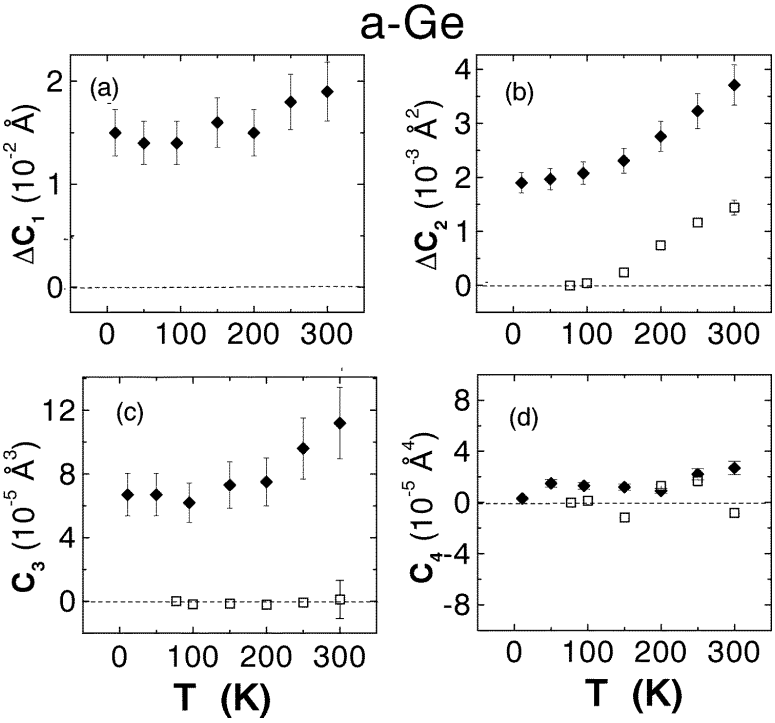

Figure 2. Cumulants of the effective first-shell distribution of the unhydrogenated a-Ge film produced by rf sputtering (diamonds). The reference for the data analysis was c-Ge at 11 K. The cumulants of c-Ge from a previous study (reference [14]) are reported for comparison (squares).

4.1. Unhydrogenated a-Ge

The temperature dependence of the cumulants of the unhydrogenated a-Ge film prepared by sputtering are shown in figure 2 (diamonds). The quality of the experimental data is better than for previous measurements on a-Ge film produced by evaporation [14]; consequently the values of the cumulants are less scattered, and more accurate conclusions will be drawn. The regular behaviour of the cumulants as a function of temperature confirms the fast convergence of the cumulant series.

In the following we will analyse the results in some detail. A detailed comparison will be made with two recent studies, one by Wakagi and Maeda [18], and the other by Filipponi and DiCicco [19]. Wakagi and Maeda have studied a sputtered a-Ge film from room temperature (r.t.) up to the crystallization temperature, analysing the EXAFS by the same procedure as was utilized in the present work, but taking r.t. c-Ge as the reference. Filipponi and DiCicco, whose main aim was to study liquid germanium, have analysed the

300 K EXAFS of an evaporated a-Ge film using phase-shifts calculated using the GNXAS package [20], and modelling the distance distribution by a Γ-like distribution.

4.1.1. Even cumulants. Let us firstly consider the second cumulant C_2, corresponding to the mean square relative displacement (MSRD) of the absorber and backscatterer atoms. The values plotted in figure 2(b) are relative to the MSRD of c-Ge at 11 K.

The difference between the a-Ge and c-Ge MSRD at low temperature gives the static contribution to the width of the first-shell distribution in a-Ge. It amounts to $\Delta\sigma^2_{stat} = (1.9 \pm 0.3) \times 10^{-3}$ Å^2 in the present case of a film produced by sputtering. This value is slightly lower than the one found by Dalba *et al* [14] for an evaporated film (2.25×10^{-3} Å^2). A difference of 2×10^{-3} Å^2 between the MSRD of a-Ge and c-Ge was found at room temperature by Wakagi and Maeda [18] for a sputtered film.

The temperature dependence of the MSRD measures the contribution due to thermal disorder. The data of figure 2(b) clearly exhibit an Einstein-like behaviour, in agreement with the results previously obtained for the evaporated a-Ge film [14]. An evaluation of the effective bond-stretching force constant can be made by considering the Einstein frequency best fitting the slope of the MSRD data. The higher the frequency, the stronger the force constant. In the present case, the Einstein frequency is $\nu = 7.22$ THz, intermediate between the frequency of c-Ge (7.5 THz) and that of evaporated a-Ge (6.9 THz) [14].

The relative comparison between the results obtained by our group using the same data reduction technique on different samples shows that both static and thermal disorder are higher in amorphous samples than in c-Ge, and also suggests that both are higher in a-Ge produced by evaporation with a substrate temperature of 160 °C than in a-Ge produced by sputtering with a substrate temperature of 220 °C.

Absolute values of the MSRD of a-Ge can be obtained by adding to the relative values of figure 2(b) the absolute value for c-Ge at 11 K. The absolute value for c-Ge can in turn be estimated by fitting an Einstein or Debye correlated model to the temperature dependence of the experimental data for c-Ge from reference [14]. A slight difference of 4×10^{-4} Å^2 is found between the Einstein and Debye models for the first shell of c-Ge [21], the Einstein model giving the higher values. Correspondingly, absolute MSRD values of $\sigma^2 = 5.3 \times 10^{-3}$ or 5.6×10^{-3} Å^2 are found for sputtered a-Ge at 300 K. A value of 5.4×10^{-3} Å^2 was determined at the same temperature by Filipponi and DiCicco [19] for an evaporated sample.

The fourth cumulant C_4 measures symmetric deviations of the distance distribution from a gaussian shape. Its values are negligibly small (figure 2(d)); a weak increase with temperature is evident nonetheless.

4.1.2. Odd cumulants. Figure 2(a) shows the differences between average values of the effective distributions of distances of a-Ge at various temperatures, and the average value of the effective distribution of the reference c-Ge at 11 K:

$$\Delta C_1 = C_1(\text{a-Ge}, T) - C_1(\text{c-Ge}, 11\ \text{K}).$$

Two features are evident: the difference $\Delta C_1 = 0.015 \pm 0.03$ Å is positive at 11 K, and it grows with temperature up to $\Delta C_1 = 0.019 \pm 0.03$ Å at 300 K.

The first cumulants of the effective and real distributions, C_1 and C_1^*, respectively, are connected through equation (1), which contains the MSRD C_2. The MSRDs are larger in a-Ge than in c-Ge because of static disorder; as a consequence, the relative values ΔC_1^* referring to the real distributions are larger than the ΔC_1 values measured directly. The ΔC_1^* values calculated through equation (1) range from 0.018 Å for a-Ge at 11 K to 0.025 Å

for a-Ge at 300 K. Our 11 K value is in good agreement with the corresponding value found by Wakagi and Maeda, comparing a-Ge with c-Ge at r.t. [18].

The average value of the real distribution is larger than the true interatomic distance, owing to the atomic displacements normal to the bond direction [22, 23, 17, 18]. If we assume that the atomic displacements normal to the bond direction are of purely thermal origin in a-Ge like in c-Ge, in view of the similarity between the effects of thermal disorder in a-Ge and in c-Ge measured by means of the Einstein frequency, we can also assume a similar increase of interatomic distances, so the difference $\Delta C_1^* = 0.018$ Å determined at 11 K should be considered the real one.

A difference in interatomic distances between a-Ge and c-Ge similar to that determined in the present work has been found by most of the structural studies on a-Ge, independently of the preparation technique, structural analysis method, and data reduction procedure. In fact, there is a good agreement between the present result and the results obtained by x-ray diffraction for evaporated a-Ge films by Temkin *et al* [24], and those obtained by neutron diffraction by Etherington *et al* [25] and by Wright *et al* [26]. The present results are also consistent with previous EXAFS data analysed by the cumulant method for evaporated films [14] and sputtered film [18], or analysed by fitting an asymmetric model distribution [19].

Table 1. The first four cumulants of the first-shell distance distributions in a-Ge and a-Ge:H of the present work are compared with other results available in the literature. All of the data are for room temperature. They have been obtained with reference to c-Ge at 11 K (present data), or at 80 K (references [7, 14]), or at r.t. (reference [8]). ΔR corresponds to ΔC_1^* of the present work. The data uncertainties relating to the present work arise from the systematic errors introduced by analysis procedures; they have been determined after using several plausible data reduction processes.

Sample	ΔR (Å)	$\Delta\sigma^2$ (10^{-3} Å^2)	C_3 (10^{-4} Å^3)	C_4 (10^{-6} Å^4)	Reference
a-Ge					
Sputtered	0.019 ± 0.003	3.71 ± 0.30	1.12 ± 0.50	2.7 ± 0.13	Present work
Sputtered	0.0160 ± 0.004	2.2 ± 0.3	2.77 ± 1.3		[8]
Sputtered	0.003(2)	1.63(10)			[7]
Evaporated	0.018 ± 0.005	4.47 ± 0.40	1.07 ± 0.42	3.52 ± 0.15	[14]
a-Ge:H					
7 at.%	0.018 ± 0.003	3.64 ± 0.30	1.06 ± 0.42	4.6±0.2	Present work
6 at.%	0.006(2)	1.10(10)			[7]
12.5 at.%	0.0110 ± 0.004	1.65 ± 0.3	2.08 ± 1.3		[8]

So, all of the recent EXAFS measurements agree with x-ray and neutron diffraction results in indicating that the first-shell distance in a-Ge is at least 0.015 Å larger than that in c-Ge. Only the first pioneering EXAFS analyses, based on the standard EXAFS formula, gave the same interatomic distance for a-Ge as for c-Ge [7, 27] (table 1). It is well established that the use of the standard EXAFS formula for asymmetric distributions gives rise to artificial reduction of interatomic distances [22].

The asymmetry of the distance distribution is measured by the third cumulant C_3, which is shown in figure 2(c) as a function of temperature. C_3 is different from zero even at very low temperature, indicating the presence of asymmetry due to static disorder. The growth of C_3 with temperature can be ascribed to asymmetry generated by anharmonicity of the thermal disorder.

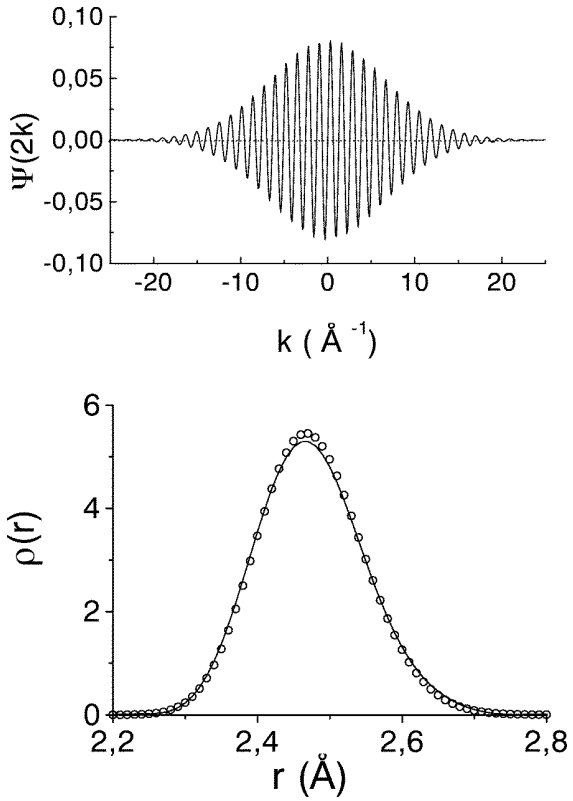

Figure 3. Upper panel: the real part of the characteristic function reconstructed from EXAFS cumulants for sputtered a-Ge measured at 300 K. Lower panel: the real part of the Fourier transform of the complex characteristic function (continuous line), compared with the distribution calculated for evaporated a-Ge by Filipponi and DiCicco [19] (dots).

4.1.3. The distribution of distances. If the cumulant series converges quickly, and EXAFS analysis yields all of the leading cumulants, it is possible to extrapolate the signal to $k = 0$, and to reconstruct the distribution of distances. This procedure was attempted for a-Ge. The characteristic function was calculated from the experimental cumulants in the k-range extending from -25 to $+25$ Å^{-1} (figure 3, upper panel). The maximum value of $|k|$ was larger than the value k_{max} for the experimental data. This choice was made on the assumption that cumulants of order higher than the fourth are negligible up to 25 Å^{-1}, so the EXAFS signal can be extrapolated not only down to $k = 0$ Å^{-1} but also up to $k = 25$ Å^{-1}. In fact, the characteristic function was regularly damped at the boundaries, and no windowing was necessary before Fourier transforming within the $\boldsymbol{k}$-range from -25 to $+25$ Å^{-1}. The real part of the Fourier transform of the characteristic function is the effective distribution of distances $P(r, \lambda)$ (the imaginary part should be zero). The real distribution of distances $\rho(r)$ was calculated from the effective one by assuming a realistic value, $\lambda = 7$ Å, for the photoelectron mean free path.

In figure 3, lower panel, the continuous line represents the real distribution of distances for one pair of nearest-neighbour atoms in sputtered a-Ge, calculated from the experimental cumulants at 300 K.

In a recent paper, Filipponi and DiCicco analysed the EXAFS of an evaporated a-Ge

sample measured at 300 K [19]. They used phase-shifts calculated by the GNXAS package, and modelled the distribution of distances by a Γ-like distribution with three free parameters: position R, variance σ^2, and skewness $\beta = C_3/\sigma^3$. The distribution of Filipponi and DiCicco, for one pair of atoms, is shown by open circles in figure 3. Only a relative shift of position of about 0.008 Å, without any normalization, was necessary to get a superposition of the two distributions. The shapes are very similar. The skewness coefficients β are 0.21 and 0.266 for the Filipponi and DiCicco distribution and ours, respectively.

It has been demonstrated that spherical wave corrections can be important in the case of asymmetric distributions [28, 29]. The analysis based on phase differences and amplitude ratios used in the present work relies on the transferability of phase-shifts and backscattering amplitudes; this could not be guaranteed when distributions of different widths and shapes are compared. The two distributions in figure 3 have been obtained by completely different methods of analysis; in particular, the GNXAS package of Filipponi and DiCicco takes into account spherical wave effects. The agreement of the two distributions shows that, at least for the degrees of disorder and asymmetry present in a-Ge at 300 K, the two methods are equivalent, and the effect of neglecting spherical wave corrections is negligible.

4.2. Hydrogenated a-Ge

The temperature dependence of the cumulants of hydrogenated a-Ge samples shows rough features very similar to those for unhydrogenated a-Ge in comparison with c-Ge: the interatomic distance, and the static and thermal contributions to the second and third cumulants are comparable for all of the amorphous samples.

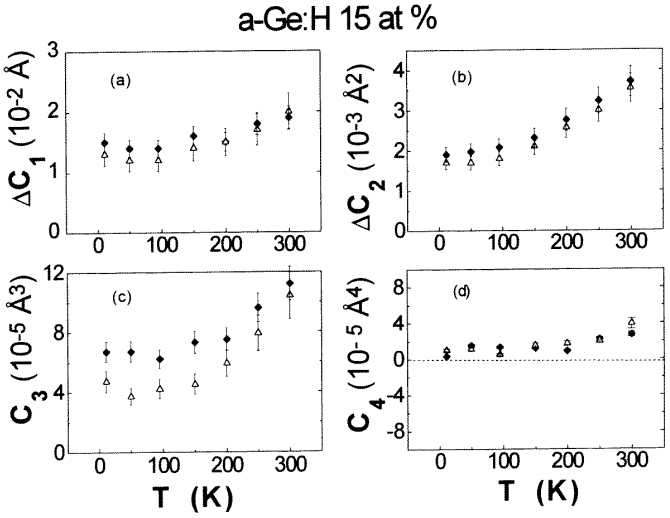

Figure 4. The first four cumulants of the first-shell distance distribution of the a-Ge:H sputtered film with 15 at.% hydrogen content (open triangles). The same data for the unhydrogenated a-Ge sputtered film (diamonds) are also shown for comparison.

However, a closer inspection reveals slight but not negligible differences between the hydrogenated samples on the one hand and the unhydrogenated one on the other, and also some modifications as a function of the hydrogen percentage. In figure 4 the first four cumulants of the sputtered a-Ge:H film with a 15 atomic per cent of hydrogen concentration

are presented (open triangles) and compared with the cumulants of the unhydrogenated a-Ge film (diamonds). The presence of hydrogen induces a slight average reduction of the interatomic distance and of the values of the second and third cumulants. A very similar behaviour is presented by the 7 and 10 at.% a-Ge:H samples.

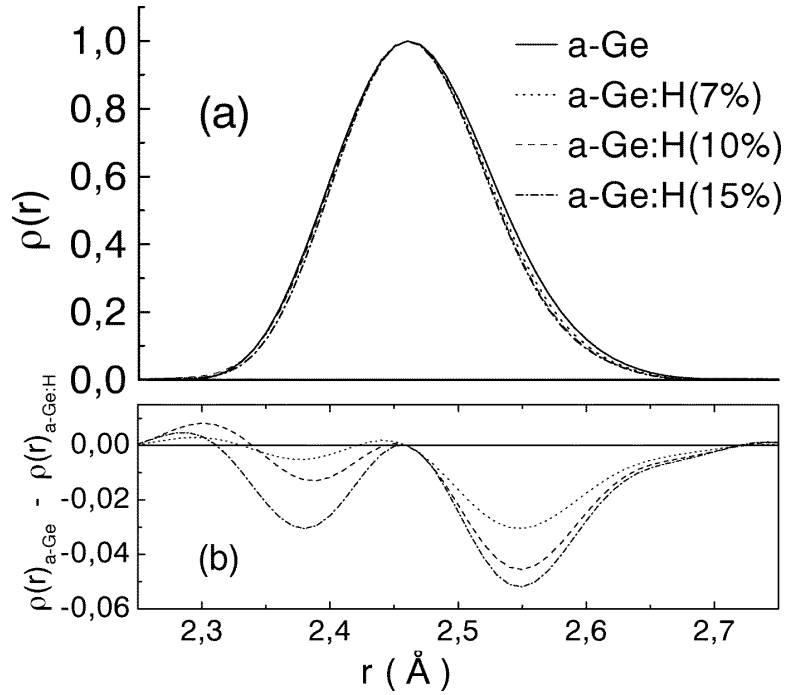

Figure 5. (a) Real distributions $\rho(r)$ of interatomic distances at $T = 11$ K reconstructed from the experimental EXAFS cumulants of a-Ge (continuous line) and a-Ge:H (dashed lines); (b) differences between the real distribution of the unhydrogenated a-Ge and those of the hydrogenated samples.

Qualitative information on the modifications induced by hydrogenation can be obtained by considering the distributions of distances reconstructed from the cumulants. The real distributions obtained by this procedure for the three hydrogenated and the unhydrogenated films at $T = 11$ K are reported in figure 5(a). The distributions become narrower and less asymmetric when the H content increases. This effect is however very weak, and can be more easily appreciated in figure 5(b), which reports the differences between the distribution of the unhydrogenated a-Ge and the distributions of the hydrogenated samples. The first four cumulants of the first-shell distance distribution in a-Ge and a-Ge:H (7 at.%) are shown in table 1, together with other results, at r.t., available in the literature. The hydrogenation process slightly influences the first-shell distance: for the a-Ge:H (7 at.%) it is 0.001 Å lower than for the a-Ge and 0.018 Å larger than for c-Ge (table 1). These results do not agree with the ones obtained by Stern and co-workers [7] who found that, for a 6 at.% hydrogenation, ΔR was 0.002 Å larger than the value for c-Ge and 0.008 Å larger than the value for a-Ge.

From EXAFS measurements we have also determined the coordination number, N, of the next-nearest neighbours of Ge atoms: we have found that, for all of the amorphous films, it is near to the value of 4 ($N = 3.95 \pm 0.12$), independently of the H content, within

an error of about 3%, according to a very conservative estimate. Such a figure is not due to insufficient counting statistics, or measurement errors, but mainly arises from the systematic errors related to the analysis procedure. Within such experimental error, this value agrees with the results of the previous EXAFS measurements, which lie between 3.79 [8] and 4 [7]. So, the present EXAFS measurements confirm previous EXAFS results [7, 14], which indicate that the nearest-neighbour coordination number is not significantly less than the value of 4 expected for tetrahedral bonding. However, these data do not agree with those obtained by means of neutron diffraction ($N = 3.68$ [26]), and the most recent ones obtained by means of reverse Monte Carlo (RMC) simulation ($N = 3.28$–3.49 [30]). This discrepancy, already discussed by Stern and co-workers [7], may be due to the fact that the EXAFS technique gives an absolute determination of the coordination number, in contrast with the diffuse scattering technique or RMC modelling, which require some assumptions about the amorphous film density.

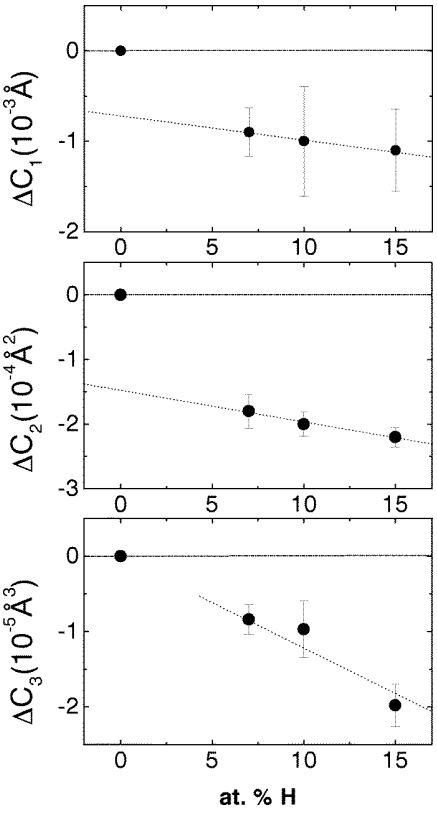

Figure 6. Difference between the first three cumulants of the hydrogenated samples and the corresponding cumulants of the unhydrogenated sample as functions of the hydrogen content. The values plotted have been obtained by averaging the differences over the temperature range explored. Error bars indicated the standard deviations of the mean distributions. The dashed lines represent linear fits of the a-Ge:H data.

Although the presence of hydrogen modifies the values of the cumulants, it does not affect their temperature dependence. In fact, very similar Einstein frequencies are obtained for all of the sputtered amorphous samples when fitting the temperature dependence of the second cumulant (table 2). We took advantage of this independence of temperature

Table 2. Einstein frequencies best fitting the temperature dependence of the MSRD of c-Ge and a-Ge samples. Amorphous samples produced by evaporation and by sputtering (hydrogenated and not) are considered.

Sample	Einstein frequency (THz)	Reference
c-Ge	7.50 ± 0.2	[14]
a-Ge (evaporated)	6.90 ± 0.2	[14]
a-Ge (sputtered)	7.22 ± 0.2	Present
a-Ge:H 7 at.%	7.16 ± 0.2	Present
a-Ge:H 10 at.%	7.25 ± 0.2	Present
a-Ge:H 15 at.%	7.12 ± 0.2	Present

by performing an accurate study of the dependence of the cumulants on the hydrogen content. To this effect, we calculated for every cumulant and for every hydrogen content the difference C_i(a-Ge:H) $-$ C_i(a-Ge) averaged over all temperatures. The results for the first three cumulants are shown in figure 6; they represent an estimate of the effects of hydrogenation on the static disorder. The difference between hydrogenated and unhydrogenated samples is sharp: the hydrogenation process produces an average reduction of about 0.001 Å (figure 4) of the interatomic distance and of 2×10^{-4} Å^2 of the MSRD (figure 4). The dependences of the interatomic distance and the MSRD on the hydrogen content are however very weak; both C_1 and C_2, after a sudden decrease caused by low H concentrations (7%), appear to decrease linearly with the hydrogen percentage. The reduction is directly proportional to the hydrogen percentage only for the third cumulant.

It is well known that a-Ge is a stressed material. The increase of the interatomic distance in unhydrogenated a-Ge with respect to that in c-Ge is a consequence of such stresses. The presence of hydrogen partially reduces the stresses of the network structure, allowing a reduction of the interatomic distances, static disorder, and asymmetry of the first-shell distance distribution.

5. Conclusions

The distribution of the first-nearest neighbours of Ge in unhydrogenated and hydrogenated a-Ge films with different H contents have been investigated by means of temperature-dependent EXAFS measurements. A cumulant analysis has been done by the phase difference and amplitude ratio method, taking c-Ge at 11 K as the reference.

For the unhydrogenated a-Ge film, the distribution of interatomic distances reconstructed from cumulants at 300 K is in good agreement with the distribution calculated by Filipponi and DiCicco through a completely different approach, based on calculated phase-shifts and amplitudes, and taking into account spherical wave corrections. The first-shell interatomic distance of the a-Ge film, prepared by sputtering, is larger than that in the crystalline Ge ($\Delta R = 0.019$ Å), as was also found for evaporated a-Ge films [14]. The nearest-neighbour coordination number of a-Ge is not significantly less than the value expected for tetrahedral bonding, in contrast with the results of some diffraction techniques and modelling calculations, which found $N \leqslant 3.7$ Å.

As for the effects of hydrogenation, the high quality of the experimental data has allowed us to detect not only the differences between the unhydrogenated sample and the hydrogenated ones, but also the slight differences between the cases of different amounts

of hydrogen. The effect of hydrogen addition to a-Ge causes the reduction of the first-shell distance, MSRD factors, and asymmetry. This general result agrees, to some extent, with the findings of previous EXAFS measurements, at room temperature, reported in the literature for similar systems; the differences, mainly concerning the absolute values of some structural parameters, can be attributed to different sample preparation conditions and/or to some inadequacies in the data analysis procedures.

The novelty of the present work lies in the determination of the first four cumulants and the reconstruction of the first-shell distance distributions as functions of temperature in the range 11–300 K. From the temperature behaviour of the Debye–Waller factors, the thermal and static disorder have been determined. No appreciable influence of the presence of H on the thermal disorder has been detected. The reduction of the static disorder that we have measured confirms that the hydrogenation process, favouring the passivation of the dangling orbitals, induces the relaxation of the amorphous network, and reduces the static disorder.

Acknowledgments

We gratefully acknowledge and thank A Traverse and F Villain for their help during the EXAFS measurements. We are also grateful to the LURE technical staff for their technical collaboration. The contribution of M Grazioli to the discussion of the data is also acknowledged.

References

[1] Chambouleyron I, Graeff C F O, Zanatta A R, Fajardo F, Mulato M, Campomanes R, Comedi D and Marques F C 1995 *Phys. Status Solidi* b **192** 241
[2] Jackson W B, Marshall J M and Moyer M D 1989 *Phys. Rev.* B **39** 1164
[3] Graeff C F O, Freire F L Jr and Chambouleyron I 1993 *Phil. Mag.* B **67** 691
[4] Paul W, Jones S J, Turner A W and Wickboldt P 1992 *J. Non-Cryst. Solids* **41** 271
[5] Evangelisti F, Proietti M G, Balzarotti A, Comin F, Incoccia L and Mobilio S 1981 *Solid State Commun.* **37** 413
[6] Stegemenn G and Lengeler B 1986 *J. Physique Coll.* **47** C8 407
[7] Bouldin C E, Stern E A, von Roedern B and Azoulay J 1984 *Phys. Rev.* B **30** 4462
[8] Wakagi M, Chigasaki M and Nomura M 1987 *J. Phys. Soc. Japan* **56** 1765
[9] Bunker G 1983 *Nucl. Instrum. Methods* **207** 437
[10] Dalba G, Fornasini P and Rocca F 1993 *Phys. Rev.* B **47** 8502
[11] Dalba G, Fornasini P, Graeff C F O, Grisenti R, Rocca F and Traverse A 1997 *Proc. 9th XAFS Conf. (Grenoble, 1996); J. Physique* at press
[12] Swanepoel R 1983 *J. Phys. E: Sci. Instrum.* **16** 1214
[13] Cardona M 1989 *Phys. Status Solidi* b **118** 463
[14] Dalba G, Fornasini P, Grazioli M and Rocca F 1995 *Phys. Rev.* B **52** 11 034
[15] Crozier E D, Rehr J J and Ingalls R 1988 *X-Ray Absorption: Principles, Applications and Techniques of EXAFS, SEXAFS and XANES* ed D C Koningsberger and R Prins (New York: Wiley) p 373
[16] Ottaviano L, DiCicco A and Filipponi A 1995 *Physica* B **208+209** 337
[17] Dalba G, Fornasini P, Gotter R and Rocca F 1995 *Phys. Rev.* B **52** 149
[18] Wakagi M and Maeda Y 1994 *Phys. Rev.* B **50** 14 090
[19] Filipponi A and DiCicco A 1995 *Phys. Rev.* B **51** 12 322
[20] Filipponi A, DiCicco A, Tyson T A and Natoli C R 1991 *Solid State Commun.* **78** 265
[21] Dalba G and Fornasini P 1997 *J. Synchrotron Radiat.* at press
[22] Eisenberger P and Brown G S 1979 *Solid State Commun.* **29** 481
[23] Ishii T 1992 *J. Phys.: Condens. Matter* **4** 8029
[24] Temkin R J, Paul W and Connel G A N 1973 *Adv. Phys.* **22** 581

[25] Etherington G, Wright A C, Wenzel J T, Dore J C, Clarke J H and Sinclair R N 1982 *J. Non-Cryst. Solids* **48** 265
[26] Wright A C, Hulme R A, Grimley D I, Sinclair R N, Martin S W, Price D L and Galeener F L 1991 *J. Non-Cryst. Solids* **129** 213
[27] Crozier E D and Seary A J 1981 *Can. J. Phys.* **59** 876
[28] Brouder C 1988 *J. Phys. C: Solid State Phys.* **21** 5075
[29] Rennert P 1992 *J. Phys.: Condens. Matter* **4** 4315
[30] Walters J K and Newport R J 1996 *Phys. Rev.* B **53** 2405